2015 IEEE/RSJ International Conference on Intelligent Robots and Systems (IROS)
Congress Center Hamburg
Sept 28 - Oct 2, 2015. Hamburg, Germany

Nonlinear modeling for a class of nano-robotic systems using piezoelectric stick-slip actuators

Tianming Lu[1], Mokrane Boudaoud[1], David Hériban[2], and Stéphane Régnier[1]

***Abstract*— This paper addresses modeling issues for a class of nano-robotic systems using piezoelectric stick-slip actuators. The work focuses on the friction force modeling to describe the dynamics of a stick-slip actuator in a wide operating range needed in nano-robotics. Based on the theory of the single state elasto-plastic model and on an experimental analysis, necessary conditions on presiding modeling are highlighted. The conditions allow describing the dynamics of stick-slip type actuators for both scanning mode and stepping mode in the time and the frequency domains and for backward and forward directions of the motion. The proposed dynamic model opens new perspective for closed loop control of nano-robotic system.**

I. Introduction

Nano-robotic systems with multiple degrees of freedom (DOF) have opened new perspectives for high precision automated tasks at very small scales [1] [2] [3]. Most of them use piezoelectric stick-slip actuators [4] because of their ability to generate millimeter displacement with a nanometer resolution [5]. A piezoelectric stick-slip actuator is made of (Fig. 1) a Piezoelectric Element (PE), a slider moving along a linear axis and a friction material between the PE and the slider. The slider is in charge of carrying a robot axis.

During a slow deformation of the PE, the friction force F_f drives the slider to a linear motion (Fig. 1(a)). After an abrupt contraction of the PE, the slider slips and cannot fully follow the sudden motion of the PE because the inertia force becomes greater than the friction force. The slip phase is illustrated in Fig. 1(b). An alternate stick and slip sequence produces a displacement of the slider relative to the PE. By repeating those operations, large range of motion of the slider can be achieved. This function mode is called *stepping mode*. The input voltage applied to the PE is a sawtooth signal so that alternate slow and abrupt deformations can be realized. If there is only stick motion without any slip, the slider can be driven with higher precision. This function mode is called *scanning mode*. The stick-slip phenomenon is determined by the physics of the contact friction force. It can be considered as the crucial part of a stick-slip actuator modeling.

Several friction force models have been proposed in the literature to describe the motion of a stick-slip actuator but they are not all suitable for nano-robotic systems. Static

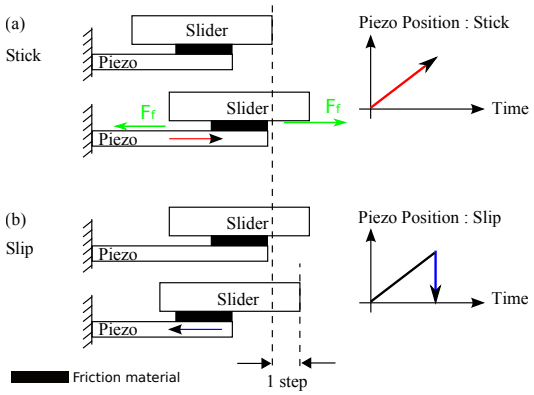

Fig. 1: Operation principle of a stick-slip actuator. (a) Stick phase; (b) Slip phase.

models describe the actuator velocity as a linear function of the input sawtooth frequency and amplitude [6]. It is a simple and efficient approximation. However, such models can only be used for stepping mode but not for scanning mode. The Coulomb friction model [7] is efficient, where the friction force is proportional to gravity. Nevertheless, if high precision positioning and low velocity tracking are required, this model can not give rise to satisfactory results [8]. In order to address the high precision positioning and tracking in nano-robotics, a comprehensive friction model must be employed to describe the phenomenon of presliding which is the motion prior to the complete slip [9]. In that sense, Swevers model [10] is able to describe complex behaviors such as presliding and hysteresis. Its complexity is a major impediment for real-time applications where computational time must be strictly controlled. The LuGre model [8] is a single-state friction model in which Stribeck effect and frictional lag are taken into account [11]. Its limitation is that it exhibits undesirable drift behavior [12].

To tackle this issue, Dupont et al. [9] have proposed a single-state elasto-plastic friction model that reduces the drift. This model has been applied in several studies [13] [5]. In most of them, the parameter of the steady-state elastic strain is taken into account as a positive constant and the model is validated in only one direction of motion. In [9], the steady-state elastic strain parameter is considered constant but it is also suggested that some parameters of the model would be changed in case of direction change. For control purposes, the model must be able to simulate the dynamic motion of the actuator in a wide operating range and for both

[1] Institut des Systèmes Intelligents et de Robotique, Université Pierre et Marie Curie, CNRS UMR 7222, 4 Place Jussieu, F-75252 Paris Cedex, France. *lu@isir.upmc.fr, mokrane.boudaoud@isir.upmc.fr, stephane.regnier@upmc.fr*
[2] Percipio Robotics, Maison des Microtechniques, 18, rue Alain Savary, 25000 Besançon, France. *david.heriban@percipio-robotics.com*

forward and backward motions.

In this paper, we tackle the issue of the dynamic modeling of piezoelectric stick-slip actuators taking into account specifications for nano-robotic systems. The aim is to study the necessary conditions of the model parameters such that:

- the model describes the dynamics of a stick-slip actuator, in time and frequency domains, for both scanning mode and stepping mode,
- the model describes the motion of the slider for both backward and forward drive directions (Fig. 2) ,
- the model must be in agreement with experiments.

We show that the aforementioned criteria can be satisfied only if specific conditions on the model parameters are taken into account. The study is based on the theory of the single state elasto-plastic model and on a series of experiments.

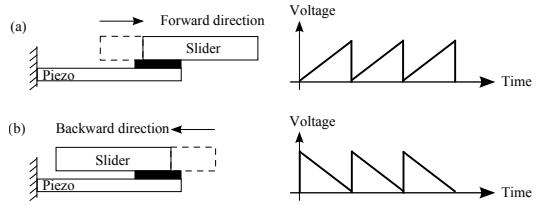

Fig. 2: Scheme showing that the direction of motion of the slider can be specified by the drive direction of the input sawtooth voltage.

II. Presentation of the Nano-Robotic System

The system is composed of a 6 DOF parallel robot and a 3 DOF Cartesian robot (Fig. 3). Each axis of the nano-robot is actuated by a piezoelectric stick-slip actuator of the same reference (SLC-1720-S-HV). The maximum stroke of the actuator is 12 mm and its resolution is in the nanometer range. The study is concerned with the dynamic modeling of the stick-slip actuator. The actuator of the Y axis in the Cartesian structure is used for the experimental validation.

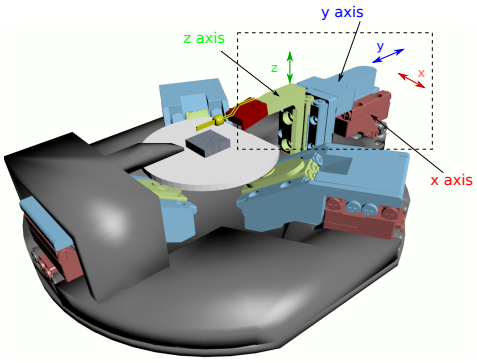

(a)

Fig. 3: CAD view of the nano-robotic system. The dashed block shows the Cartesian 3 DOF (XYZ) nano-robotic part.

III. Nonlinear Dynamic Modeling

For the dynamic modeling of the nano-robotic system, an accurate dynamic model of an elementary actuator is needed. The major impediment lies in the fact that the internal structure is no public information. As such, three main assumptions are made (Fig. 4): (i) the PE is attached to the base of the actuator, (ii) the slider is guided by a linear crossed roller guideway and has only one translational DOF, (iii) there is no lubricant between the slider and the PE.

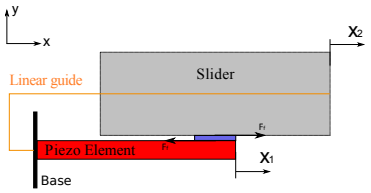

(a)

Fig. 4: Scheme of the piezoelectric stick-slip actuator.

A. Dynamic Modeling of the PE and the slider

1) Dynamic Modeling of the PE: The dynamic of the PE can be described by a second order differential equation:

$$M_p \frac{d^2x_1}{dt^2} + D_p \frac{dx_1}{dt} + K_p x_1 = K_{act1} U - K_{act2} N - F_f \quad (1)$$

x_1 is the deformation of the PE along x axis in response to an input voltage U. M_p, D_p and K_p are respectively the mass, the damping and the stiffness of the PE. N is the normal force applied by the slider to the PE. F_f is the friction force. K_{act1} and K_{act2} are static gains.

The PE is also characterized by the creep and the hysteresis [14]. The creep is a slow phenomenon and is therefore not considered in this study. The hysteresis is analyzed in scanning mode. Experimental results (see section IV-B.2) have shown that the hysteresis is rate-dependent. Its shape depends on the input signal frequency. However, the hysteresis does not modify the resonance frequencies. In such a case, the dynamic hysteresis can be modeled as a static hysteresis $H(U)$ followed by a linear dynamic part of the PE whose static gain is equal to 1 [15]. The static hysteresis $H(U)$ can then be introduced in equation (1) as follows:

$$M_p \frac{d^2x_1}{dt^2} + D_p \frac{dx_1}{dt} + K_p x_1 = K_p H(U) U - K_{act2} N - F_f \quad (2)$$

The Prandtl-Ishlinskii (PI) static Hysteresis model is used to describe $H(U)$. Each element of the PI model is a backlash characterized by a bandwidth and a weighting coefficient [16]. Identification results of the hysteresis are presented in section IV-B.2.

B. Modeling of the Slide

Theoretically, the only external excitation that drives the slider is the friction force F_f. It is due to the relative motion $x_1 - x_2$ between the PE and the slider (see Fig. 4). The dynamic equation of the slider can be governed as follows:

$$M_s \frac{d^2x_2}{dt^2} + D_s \frac{dx_2}{dt} = F_f \quad (3)$$

M_s is the mass of the slider and D_s is a damping parameter. The dynamic equation of the PE and that of the slider will be coupled taking into account the friction force.

C. Modeling of the Friction

In order to define the dynamic transfer function between the displacement of the slider x_2 and the input voltage U, the friction force F_f must be modeled. The single-state elasto-plastic friction model [9] is used in this work.

The relative motion $x = x_1 - x_2$ between the PE and the slider is decomposed into elastic (reversible) and plastic (irreversible) components, denoted by z and w respectively:

$$x = z + w \tag{4}$$

The elasto-plastic friction force F_f is governed by the following equation:

$$F_f = \rho_0 z + \rho_1 \dot{z} + \rho_2 \dot{x} \tag{5}$$

ρ_0, ρ_1 and ρ_2 are respectively the contact stiffness, the damping for the tangential compliance and the viscous friction constant. The viscous friction force $\rho_2 \dot{x}$ is considered negligible compared to dry friction. This is the case when the frictional phenomenon is presliding dominant with a small relative velocity $\dot{x}$ [17].

The elastic component z is governed by:

$$\dot{z} = \dot{x}\left[1 - \alpha(z, \dot{x})\frac{z}{z_{ss}}\right] \tag{6}$$

z_{ss} is the steady-state elastic strain which is often considered constant [13].

The continuous function $\alpha(z, \dot{x})$ is defined by equation (7), with:

$$\alpha\,(.) = \frac{1}{2} Sin\left(\pi \frac{z - \frac{z_{ss}+z_{ba}}{2}}{z_{ss} - z_{ba}}\right) + \frac{1}{2} \tag{8}$$

$z_{ba} > 0$ is the break-away displacement.

The model behaves elastically when $|z| < z_{ba}$. When $|z|$ is between z_{ba} and $|z_{ss}|$, mixed elastic and plastic displacements are produced. If $|z|$ is equal to $|z_{ss}|$, only a plastic displacement or sliding occurs.

z_{ss} is often assigned as a positive constant independent of $\dot{x}(t)$. In this case, we will show that the model can only simulate one direction of motion which is problematic for control purposes (e.g. tracking of a sinusoid trajectory).

> ***Proof***: Consider a general working scenario where x evolves along only one direction from zero initial conditions. Elasto-plastic presliding begins with pure elastic, evolves then to mixed and finally to plastic displacements. In pure elastic regime, $\alpha(z, \dot{x})$ is zero so that $\dot{z} = \dot{x}$. This equality assures that the elastic strain is consistent with the motion direction. Once $|z|$ goes beyond the break-away threshold z_{ba}, mixed displacements occur. If z_{ss} is kept constant, there will be one motion direction so that $\frac{z(t)}{z_{ss}} < 0$, e.g. the motion is driven in the negative direction (backward) while z_{ss} is a positive constant. Given the condition $0 < \alpha(z, \dot{x}) < 1$ from (8) in the mixed regime, it leads to (9):
>
> $$1 - \alpha(z, \dot{x})\frac{z(t)}{z_{ss}} > 1, \quad \text{if } \operatorname{sgn}(z(t)) \neq \operatorname{sgn}(z_{ss}) \tag{9}$$
>
> Let us denote $C = 1 - \alpha(z, \dot{x})\frac{z(t)}{z_{ss}}$. By taking the derivative of (4) and combining with (6), it yields:
>
> $$\dot{z} = \dot{x} - \dot{w} = C\dot{x} \tag{10}$$
>
> $$\dot{w} = (1 - C)\dot{x} \tag{11}$$
>
> Since $1 - C < 0$, thus:
>
> $$\operatorname{sgn}(\dot{w}) \neq \operatorname{sgn}(\dot{x}) \tag{12}$$
>
> According to [9], this inequality occurs only in the case of elastic super relaxation following motion reversal. This is not in accordance with the working scenario where the motion evolves along only one direction. As a result, keeping z_{ss} a constant cannot address the need of modeling backward and forward motions.

In the sequel, z_{ss} is denoted $z_{ss}(\dot{x})$. It is determined by the steady-state friction force $f_{ss}(\dot{x})$ in equation (13):

$$z_{ss}(\dot{x}) = \begin{cases} \frac{f_{ss}(\dot{x})}{\rho_0}, & \text{if } |\dot{x}| > 0 \\ \lim_{\dot{x}\to 0+}\left[\frac{f_{ss}(\dot{x})}{\rho_0}\right], & \text{if } \dot{x} = 0 \end{cases} \tag{13}$$

In [18], an efficient modeling of the steady-state force is proposed:

$$f_{ss}(\dot{x}) = \left[(f_{max} - f_c)\frac{1}{1 + (\frac{\dot{x}}{v_s})^2} + f_c\right]\operatorname{sgn}(\dot{x}) \tag{14}$$

f_c is the Coulomb friction, f_{max} is the maximum static friction amplitude, and v_s is the characteristic velocity.

Without considering the Stribeck effect [8], one straight forward solution is to change the sign of z_{ss} with respect to the relative motion $\dot{x}$ direction. i.e.:

$$z_{ss}(\dot{x}) = \begin{cases} \frac{f_c \operatorname{sgn}(\dot{x})}{\rho_0}, & \text{if } |\dot{x}| > 0 \\ \frac{f_c}{\rho_0}, & \text{if } \dot{x} = 0 \end{cases} \tag{15}$$

This is a special case in the Stribeck steady-state friction formula with f_{max} being equal to f_c in (14). The Stribeck effect is not considered but the motion direction is taken into account. The steady-state friction force is then reduced to:

$$f_{ss}(\dot{x}) = f_c \operatorname{sgn}(\dot{x}) \tag{16}$$

The friction force F_f is modeled using equations (4), (5), (6), (7), (8) and (15). Dynamic models of the PE and the slider can be coupled taking into account the friction model. In scanning mode, the actuator behaves like a coupled oscillator.

IV. Experimental Analysis and Identification

A. Description of the experimental setup

The experimental setup is composed of: (i) the nano-robotic system, (ii) the laser interferometer (resolution: 0.1 nm), (iii) a vibration isolation table and (iv) a controller board with a Real Time Interface (RTI). The interferometer and the nano-robot are set in two different vibration isolation tables to avoid the transmission of the actuator vibrations to the laser sensor. The laser of interferometer is aligned to measure the displacement of the Y axis of the Cartesian structure (Fig. 5). Measurements are performed with 25 kHz sampling frequency. The nano-robotic system is interfaced to a host computer via the controller board.

$$\alpha(z,\dot{x}) = \left\{ \begin{array}{ccc} 0 & if & |z| \leqslant z_{ba} \\ 0 < \alpha(.) < 1 & if & z_{ba} < |z| < |z_{ss}| \\ 1 & if & |z| \geqslant |z_{ss}| \end{array} \right\} \quad if \quad \mathrm{sgn}(\dot{x}) = \mathrm{sgn}(z)$$
$$0 \qquad\qquad if \quad \mathrm{sgn}(\dot{x}) \neq \mathrm{sgn}(z) \tag{7}$$

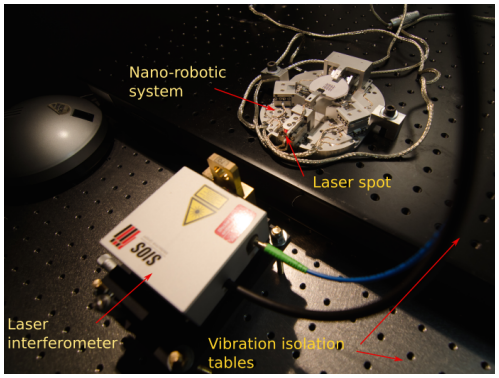

Fig. 5: Experimental setup for model identification. The interferometer laser is aligned to perform measurements of the position of the Y axis.

B. Parameters identification

The identification of the parameters has been performed in three steps:

1) ***Step1*** *- Parameters identification in scanning mode-:* A 40 V step voltage is applied to the actuator (Y axis). The measured displacement of the slider and its Power Spectral Density (PSD) are shown in Fig. 6(a) and Fig. 6(b) respectively. The PSD shows two resonant modes at 595 Hz and 1633 Hz and an antiresonance at 725 Hz. In the theory of coupled oscillators, the antiresonance can be observed only in the frequency spectrum of the driven oscillator.

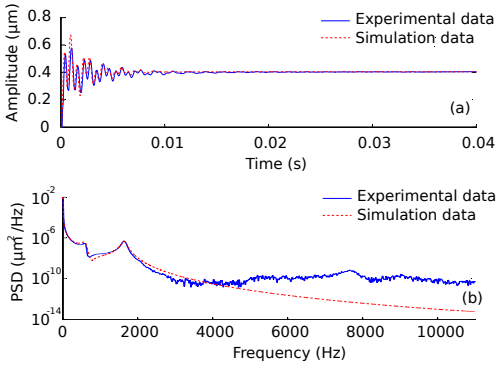

Fig. 6: Step response of the stick-slip actuator for a 40 V step excitation (a) and PSD of step response (b). Simulation and experimental results.

In the case of stick-slip actuators, the driven oscillator is the PE and the undriven oscillator is the slider. The antiresonance can only appear for the dynamic transfer x_1/U. However, the interferometer sensor measures the displacement of the slider. As such, experimental results of Fig. 6(b) demonstrate that the measured displacement is a combination of x_1 and x_2. This is consistent because the vibrations of the PE are also transmitted to the slider through the linear guide (see Fig. 4). We therefore consider U and $q = x_1 + x_2$ respectively as the input and the output of the stick-slip dynamic model.

The measured step response of Fig. 6(a) is used for the identification of the dynamic parameters of the PE and the slider. Results are: $M_p = 2.47 \times 10^{-4}$ $[Kg]$, $D_p = 15.6125$ $[Ns/\mu m]$, $K_p = 2.62 \times 10^6$ $[N/\mu m]$, $M_s = 0.0247$ $[Kg]$, $D_s = 64.9651$ $[Ns/\mu m]$, $\rho_0 = 3.517 \times 10^5$ $[N/\mu m]$ and $\rho_1 = 0$. K_{act2} is set at 1200.

2) ***Step2*** *- identification of the hysteresis in scanning mode-:* The PI hysteresis model has been identified as follows: (i) A sine input voltage is applied to the actuator. The amplitude and the frequency of the sine signal are 40 V and 50 Hz respectively. The position of the slider in response to the sine voltage is measured experimentally. (ii) The experimental hysteresis curve is shifted in the positive section of the $[U, q]$ plane. (iii) $n = 35$ elementary backlashes are defined. (iv) The input U is split into $n+1$ non uniform partitions. The bandwidth of each elementary backlash is defined. (v) The weighting coefficient of each backlash is then identified. See [16] for more details about the PI identification method.

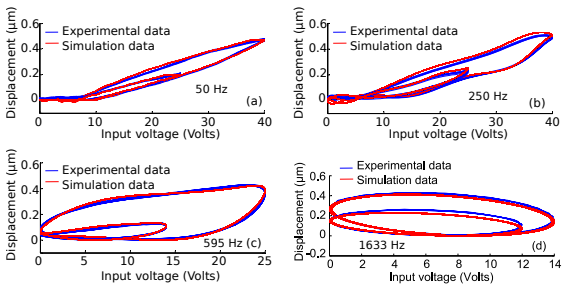

Fig. 7: Experimental and simulation results of the identified PI model for different frequencies of the input sine signal: (a) 50 Hz, (b) 250 Hz, (c) 595 Hz and (d) 1633 Hz.

Taking into account the dynamic model of the stick-slip actuator and the PI hysteresis model, the hysteresis curve of the system q/U has been simulated. Results have been compared with experimental measurements (Fig. 7).

3) ***Step3*** *- identification of the break-away elastic strain and the steady-state elastic strain in stepping mode:* The stick-slip actuator is driven by sawtooth signals. The velocity $\dot{q}$ (slope of the displacement) can be measured given a sequence of sawtooth with varying frequencies and amplitudes in both drive directions. This measurement is used to identify the break-away elastic strain z_{ba} and the steady-state elastic strain $|z_{ss}|$ so that the velocity matches between the model and experimental data. The ratio between z_{ba} and $|z_{ss}|$ has been kept constant $z_{ba}/|z_{ss}| = 0.667$.

The break-away elastic strain z_{ba} depends on input signal

properties (amplitude and frequency of the sawtooth signal). The friction force F_f must vary to take into account input sawtooth signals of different properties. Since the parameter ρ_0 must be kept constant to ensure the frequency response of Fig. 6(b), the parameters z_{ba} must vary to take into account input sawtooth of different frequency and amplitude. See equations (5), (6), (7) and (8). Fig. 8 illustrates the evolution of the identified z_{ba} versus the amplitude of an input sawtooth signal of 50 Hz frequency. In the figure, $z_{ba}(-)$ and $z_{ba}(+)$ denote respectively the value of z_{ba} for backward and forward motion directions of the slider.

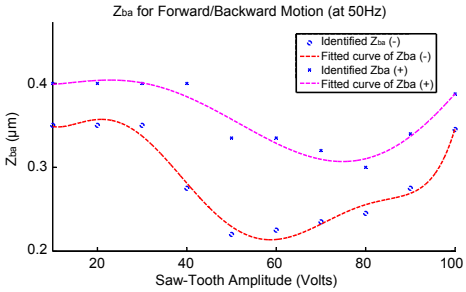

Fig. 8: Characteristic of the break-away elastic strain versus input sawtooth amplitude. The sawtooth frequency is 50 Hz.

C. Model Validation

The model (i.e. dynamic transfer q/U) is validated with experiments. For both scanning mode and stepping mode, the input voltage is a sawtooth signal. Three input frequencies are used for the validation: 50, 100 and 500 Hz.

In scanning mode, the input amplitude is equal to 20 V. Results of Fig. 9 show that the output q of the dynamic model returns back at its initial position after the abrupt drop of the voltage. For different frequencies of the input sawtooth voltage, the model works in scanning mode. This is in agreement with experimental data.

In stepping mode, two input sawtooth voltages of 40 and 60 V in amplitude are used. The model is validated with experiments in the time domain and in the frequency domain. Results of Fig. 10 show that for an input voltage of 40 V, the actuator behaves in a stick and slip operating mode. The velocity of the slider increases with increasing the amplitude of the input voltage. This can be observed for instance by comparing Fig. 10 (a) with Fig. 10 (d), Fig. 10 (b) with Fig. 10 (e) and Fig. 10 (c) with Fig. 10 (f). Moreover, experiments show that the velocity of the slider is different in forward and backward operating modes. The model describes accurately this "asymmetric" behavior.

To validate the dynamic model in the frequency domain for both scanning mode and stepping mode, the PSD of the model output is computed for two different input sawtooth signals: (20 V, 500 Hz) and (40 V, 50 Hz). Fig. 11 shows experimental and simulation results in frequency domain.

V. Discussion

In this study, the Stribeck effect [8] is not considered since no lubricant film is assumed to exist between friction

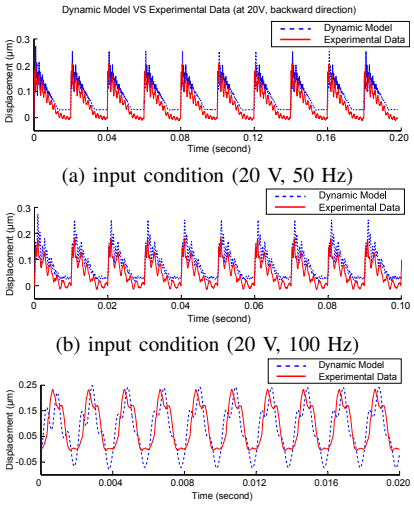

(a) input condition (20 V, 50 Hz)

(b) input condition (20 V, 100 Hz)

(c) input condition (20 V, 500 Hz)

Fig. 9: Comparison in the time domain between experimental and simulation data for different input sawtooth conditions.

surfaces. In the literature, the steady-state elastic strain is often kept as a positive constant. In this paper, it has been shown that such an assumption cannot fulfill the condition to simulate the motion of the slider in both backward and forward directions. The steady-state elastic strain must vary to consider the drive direction. The experiments have shown the asymmetric behavior of the slider requiring a model identification for both drive directions.

In the case of the discrete computation of the elasto-plastic friction model [18], the elastic strain $\hat{z}(k)$ is suggested to be saturated by $z_{ss}(k)$. Even if the model is designed in a continuous form, the saturation condition must be introduced.

The break-away elastic strain z_{ba} must be identified for different amplitudes and frequencies of the input sawtooth signal. The friction force is dependent on these operating conditions. The evolution of z_{ba} versus the amplitude of the input signal has been identified through experiments (Fig. 8) for a fixed frequency. In order to control in closed loop the position of the slider in stepping mode, the PE can be actuated by a sawtooth signal with controlled amplitude and frequency. New control strategies can be developed in the future if the identification of z_{ba} is performed in the workspace including the frequency and the voltage amplitude of the driving signal and the motion direction. This will lead to the extension of the result of Fig. 8 into a surface fitting.

VI. Conclusions

Piezoelectric stick-slip is one of the main actuation principle for nano-robotic systems. It allows positioning the nano-robotic axis in the millimeter range with a nanometer resolution. This paper has dealt with modeling issues for this class of robotic systems. In particular, the work has focused on the proposition of a modeling approach being able to describe the motion of a stick-slip actuator in varying operating conditions. Due to the complexity of the presiding, it is hard to develop a single model which reflects the

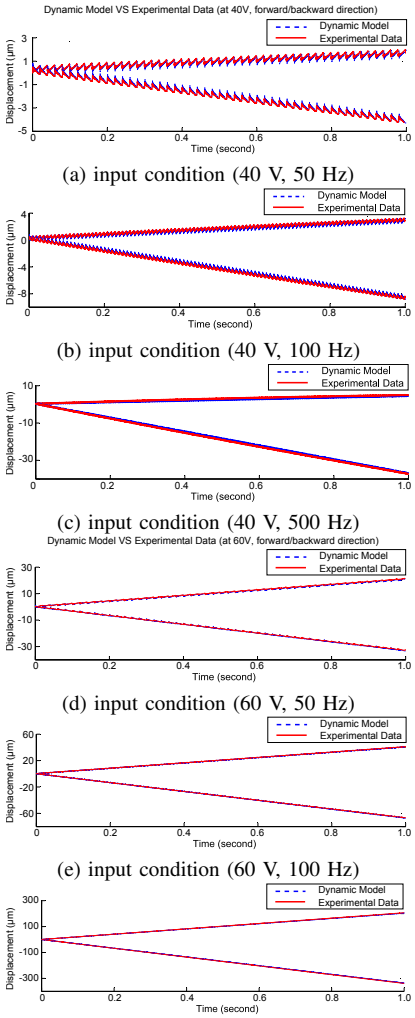

(a) input condition (40 V, 50 Hz)

(b) input condition (40 V, 100 Hz)

(c) input condition (40 V, 500 Hz)

(d) input condition (60 V, 50 Hz)

(e) input condition (60 V, 100 Hz)

(f) input condition (60 V, 500 Hz)

Fig. 10: Comparison in the time domain between experimental and simulation data for different input sawtooth condition.

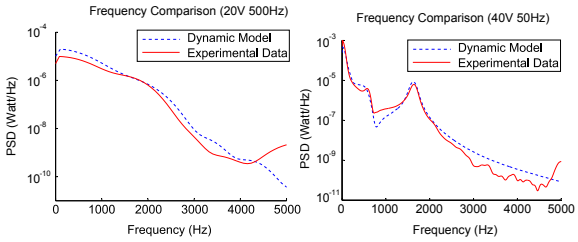

(a) input condition (20V 500Hz) (b) input condition (40V 50Hz)

Fig. 11: Comparison in the frequency domain between experimental and simulation data for different input sawtooth conditions.

dynamics of such systems for both scanning mode and stepping mode in the time and the frequency domains and for backward and forward directions of the motion. Necessary conditions on the model parameters have been obtained to meet such specifications. The proposed modeling approach has been validated with a series of experiments. In our best knowledge, the validation of stick-slip actuator model in such operating conditions has never been demonstrated in the literature. Future works will concern the closed loop control of the studied nano-robotic system for speed automated tasks inside a Scanning Electron Microscope (SEM).

VII. Acknowledgment

This work has been supported by the projects "SimRap" (CNRS défi Instrumentation aux limites 2015) and NanoRobust (ANR 2011 NANO 006). The authors would like to thank Percipio Robotics for their support.

References

[1] Y. L. Zhang, Y. Zhang, C. Ru, B. Chen, and Y. Sun, "A load-lock-compatible nanomanipulation system for scanning electron microscope," *Mechatronics, IEEE/ASME Transactions on*, vol. 18, no. 1, pp. 230–237, Feb 2013.

[2] E. C. Heeres, A. J. Katan, M. H. van Es, A. F. Beker, M. Hesselberth, D. J. van der Zalm, and T. H. Oosterkamp, "A compact multipurpose nanomanipulator for use inside a scanning electron microscope," *Review of Scientific Instruments*, vol. 81, no. 2, 2010.

[3] SmarAct, "http://www.smaract.de/," 2014.

[4] N. Chaillet and S. Régnier, Eds., *Microrobotics for Micromanipulation*. Wiley-ISTE, 2010.

[5] M. Rakotondrabe, Y. Haddab, and P. Lutz, "Development, modeling, and control of a micro-/nanopositioning 2-dof stick-slip device," *Mechatronics, IEEE/ASME Transactions on*, vol. 14, no. 6, pp. 733–745, Dec 2009.

[6] A. Bergander and J.-M. Breguet, "Performance improvements for stick-slip positioners," in *Micromechatronics and Human Science, 2003. MHS 2003. Proceedings of 2003 International Symposium on*, Oct 2003, pp. 59–66.

[7] S. Chang and S. Li, "A high resolution long travel friction-drive micropositioner with programmable step size," *Review of Scientific Instruments*, vol. 70, no. 6, pp. 2776–2782, Jun 1999.

[8] C. C. De Wit, H. Olsson, K. J. Astrom, and P. Lischinsky, "A new model for control of systems with friction," *Automatic Control, IEEE Transactions on*, vol. 40, no. 3, pp. 419–425, 1995.

[9] P. Dupont, V. Hayward, B. Armstrong, and F. Altpeter, "Single state elastoplastic friction models," *Automatic Control, IEEE Transactions on*, vol. 47, no. 5, pp. 787–792, 2002.

[10] J. Swevers, F. Al-Bender, C. Ganseman, and T. Projogo, "An integrated friction model structure with improved presliding behavior for accurate friction compensation," *Automatic Control, IEEE Transactions on*, vol. 45, no. 4, pp. 675–686, Apr 2000.

[11] B. Zhong, L. Sun, L. Chen, and Z. Wang, "The dynamics study of the stick-slip driving system based on lugre dynamic friction model," in *Mechatronics and Automation (ICMA), 2011 International Conference on*, Aug 2011, pp. 584–589.

[12] V. Hayward and B. Armstrong, "A new computational model of friction applied to haptic rendering," in *Experimental Robotics VI*. Springer, 2000, pp. 403–412.

[13] J. Peng and X. Chen, "Modeling of piezoelectric-driven stick-slip actuators," *Mechatronics, IEEE/ASME Transactions on*, vol. 16, no. 2, pp. 394–399, April 2011.

[14] G. Gu, L. Zhu, C. Su, H. Ding, and S. Fatikow, "Modeling and control of piezo-actuated nanopositioning stages: A survey," *Automation Science and Engineering, IEEE Transactions on*, vol. PP, no. 99, pp. 1–20, 2014.

[15] M. Rakotondrabe, Y. Haddab, and P. Lutz, "Quadrilateral modelling and robust control of a nonlinear piezoelectric cantilever," *Control Systems Technology, IEEE Transactions on*, vol. 17, pp. 528–539, 2009.

[16] M. Rakotondrabe, C. Clevy, and P. Lutz, "Complete open loop control of hysteretic, creeped, and oscillating piezoelectric cantilevers," *Automation Science and Engineering, IEEE Transactions on*, vol. 7, no. 3, pp. 440–450, July 2010.

[17] F. Landolsi, F. H. Ghorbel, J. Lou, H. Lu, and Y. Sun, "Nanoscale friction dynamic modeling," *Journal of dynamic systems, measurement, and control*, vol. 131, no. 6, p. 061102, 2009.

[18] V. Hayward, B. Armstrong, F. Altpeter, and P. E. Dupont, "Discrete-time elasto-plastic friction estimation," *Control Systems Technology, IEEE Transactions on*, vol. 17, no. 3, pp. 688–696, 2009.